ELSEVIER

Signal Processing 57 (1997) 251–270

SIGNAL PROCESSING

# Orthonormal shift-invariant wavelet packet decomposition and representation

Israel Cohen*, Shalom Raz, David Malah

*Department of Electrical Engineering, Technion – Israel Institute of Technology, Technion City, Haifa 32000, Israel*

Received 15 January 1996; revised 15 August 1996

**Abstract**

In this work, a shifted wavelet packet (SWP) library, containing all the time shifted wavelet packet bases, is defined. A corresponding shift-invariant wavelet packet decomposition (SIWPD) search algorithm for a 'best basis' is introduced. The search algorithm is representable by a binary tree, in which a node symbolizes an appropriate subspace of the original signal. We prove that the resultant 'best basis' is orthonormal and the associated expansion, characterized by the lowest information cost, is shift-invariant. The shift invariance stems from an additional degree of freedom, generated at the decomposition stage and incorporated into the search algorithm. The added dimension is a relative shift between a given parent node and its respective children nodes. We prove that for any subspace it suffices to consider one of two alternative decompositions, made feasible by the SWP library. These decompositions correspond to a zero shift and a $2^{-\ell}$ relative shift where $\ell$ denotes the resolution level. The optimal relative shifts, which minimize the information cost, are estimated using finite depth subtrees. By adjusting their depth, the quadratic computational complexity associated with SIWPD may be controlled at the expense of the attained information cost down to $O(N \log_2 N)$. © 1997 Elsevier Science B.V.

**Zusammenfassung**

In dieser Arbeit wird eine Bibliothek von Zeitverschiebungs-Waveletpaketen (SWP) definiert, die sämtliche zugehörigen SWP-Basen enthält. Ferner wird ein entsprechender Suchalgorithums für die verschiebungsinvariante Waveletpaketzerlegung (SIWPD) zur Bestimmung der 'optimalen Basis' vorgestellt. Als Optimierungskriterium wird dabei eine Informations-Kostenfunktion benutzt. Der Algorithmus läßt sich als binärer Baum darstellen, bei dem die Knoten geeignete Unterräume des ursprünglichen Signals symbolisieren. Wir zeigen, daß die resultierende 'optimale Basis' orthonormal und die mit Hilfe dieser Basis gewonnene Darstellung des Signals verschiebungsinvariant ist. Diese Signalzerlegung ist durch die geringsten Informations-Kosten charakterisiert. Die Verschiebungsinvarianz resultiert aus einem zusätzlichen Freiheitsgrad, der sich während der Zerlegungsphase ergibt und im Suchalgorithmus mitberücksichtigt wird. Die zusätzliche Dimension entspricht einer relativen Verschiebung zwischen einem gegebenen Elternknoten und seinem zugehörigen Kindknoten. Wir zeigen, daß es mit Hilfe der erstellten SWP-Bibliothek für jeden beliebigen Unterraum hinreichend ist, lediglich ein oder zwei alternative Zerlegungen in Betracht zu ziehen. Diese Zerlegungen entsprechen einer Nullverschiebung und einer relativen Verschiebung von $2^{-\ell}$ Elementen, wobei $\ell$ den Auflösungsgrad bezeichnet. Die optimalen relativen Verschiebungen, die das Informationskostenkriterium minimieren, werden durch Unterbäume endlicher Tiefe geschätzt. Durch Veränderung ihrer Tiefe kann die quadratische Rechenkomplexität der SIWPD auf Kosten der erzielten Informationsgüte auf die Ordnung $N \log_2 N$ reduziert werden. © 1997 Elsevier Science B.V.

*Corresponding author. E-mail: cisrael@rotem.technion.ac.il.


*PII* S0165-1684(97)00007-8

**Résumé**

Dans ce travail, nous définissons une librairie de paquets d'ondelettes décalées (POD), contenant toutes les bases de paquets d'ondelettes décalées en temps. On introduit ensuite l'algorithme correspondant de recherche de décomposition en paquets d'ondelettes invariants en décalage (DPOID) pour trouver la 'meilleure base'. L'algorithme de recherche peut être représenté par un arbre binaire, dans lequel chaque noeud symbolise un sous-espace du signal original. Nous prouvons que la 'meilleure base' résultante est orthonormale, et que l'expansion associée, charactérisée par le coût informationnel le plus bas, est invariante en décalage. Cette invariance provient d'un degré de liberté supplémentaire, généré au moment de la décomposition et incorporé dans l'algorithme de recherche. La dimension ajoutée est un décalage relatif entre un noeud-parent donné et ses noeuds-enfants respectifs. Nous prouvons que pour tout sous-espace il suffit de considérer l'une des deux décompositions alternatives, rendues possibles grâce à la libraire POD. Ces décompositions correspondent à un décalage de zéro et un décalage relatif de $2^{-\ell}$ où $\ell$ est le niveau de résolution. Les décalages relatifs optimaux, qui minimisent le coût informationnel, sont estimés en utilisant des sous-arbres de profondeur finie. En ajustant leur profondeur, la complexité de calcul quadratique associée à la DPOID peut être réduite, au prix du coût informationnel final, à $O(N \log_2 N)$. 

*Keywords*: Shift-invariant; Best basis; Time frequency; Wavelets; Wavelet packets; Algorithm; Translation

## 1. Introduction

Wavelet packets (WP) were first introduced by Coifman and Meyer [12] as a library of orthonormal bases for $L^2(\mathbb{R})$. The proposed library, generated via a generalized version of the multiresolution decomposition [13, 31], is cast into a binary tree configuration, in which the nodes represent subspaces with different time-frequency localization characteristics [15]. The library encompasses as special cases both octave band (wavelet) as well as uniform filter-bank representations (Fig. 1) [45].

Implementation of a *best basis* selection procedure for a prescribed signal (or a family of signals) requires the introduction of an acceptable *cost function* which translates 'best' into a minimization process. A decisive simplification takes place whenever the cost function is of an additive nature as is the case when 'entropy' [15, 48] or rate-distortion [38] criteria are used. The efficiency associated with the minimization of additive cost functions are intimately linked to the computationally efficient determination of an optimal tree decomposition. Specifically, at each resolution level, further decomposition of a given parent node is carried out based exclusively on a local cost function reduction. The orthonormality of the representation together with the additivity of the cost function render the decomposition of a prescribed node independent of any other node at the same resolution level. The 'best' decomposition tree is obtained recursively on a complexity level $O(NL)$ [15], where $N$ is the signal length at its highest resolution level, and $L$ denotes the number of decomposition levels ($L \leqslant \log_2 N$).

The cost function selection is closely related to the specific nature of the application at hand. Entropy, for example, may be used to effectively measure the energy concentration of the generated nodes [16, 26, 47]. Statistical analysis of the best-basis coefficients may provide a characteristic time-frequency signature of the signal, potentially useful in simplifying identification and classification applications [6, 28]. A major deficiency of this approach is the lack of shift invariance. Both the wavelet packet decomposition (WPD) and local cosine decomposition (LCD) of Coifman and Wickerhauser [15], as well as the extended algorithms proposed by Herley et al. [23, 24], are sensitive to the signal location with respect to the chosen time origin.

Shift-invariant multiresolution representations exist. However, some methods either entail high oversampling rates (e.g., in [4, 5, 27, 39, 42], no down sampling with the changing scale is allowed) or immense computational complexity (e.g., the *matching pursuit* algorithm [35, 20]). In some other methods, the resulting representations are

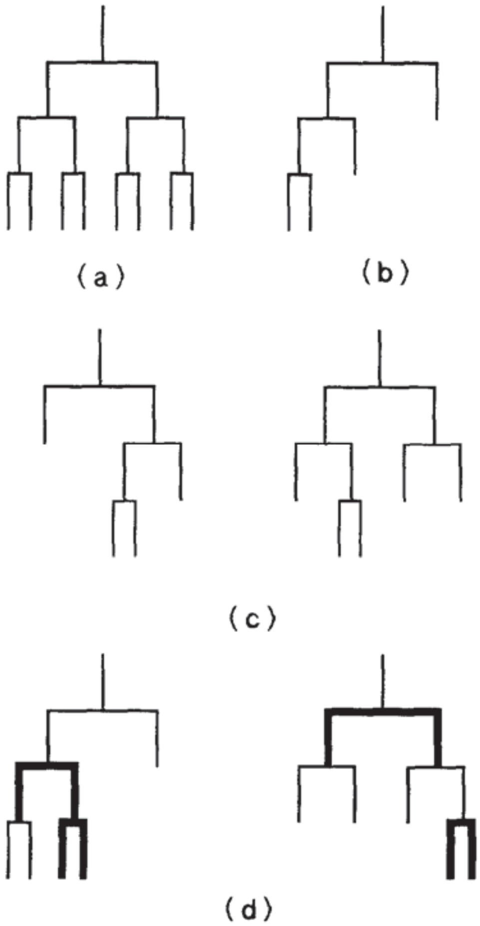


Fig. 1. Three-level expansions trees: (a) the short-time Fourier transform, (b) the wavelet transform, (c) typical expansion trees of Wavelet Packet Decomposition (WPD), (d) typical expansion trees of shift-invariant wavelet packet decomposition (SIWPD).

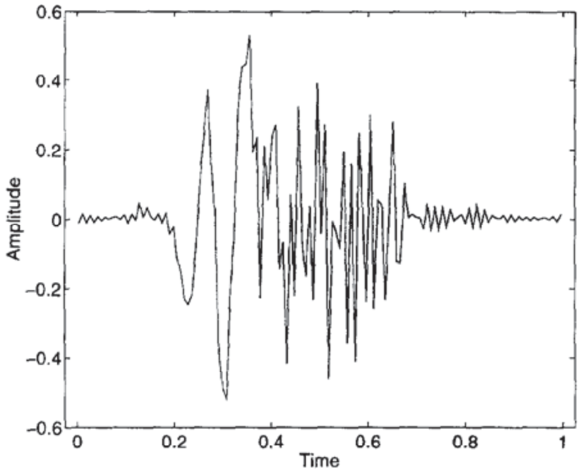


Fig. 2. Test signal $g(t)$.

non-unique and involve approximate signal reconstructions, as is the case for zero crossing or local maxima methods [3, 25, 32–34]. Another approach has given up obtaining shift invariance and settled for a less restrictive property named *shiftability* [1, 43], which is accomplished by imposing limiting conditions on the scaling function [1, 2, 46].

Recently, several authors proposed independently to extend the library of bases, in which the best representations are searched for, by introducing additional degrees of freedom that adjust the time-localization of the basis functions [8, 9, 11, 22, 29, 37]. It was proved that the proposed modifications of the wavelet transform and wavelet packet decomposition lead to orthonormal best-basis representations which are shift invariant and are characterized by lower information costs. The principal idea is to adapt the down sampling when expanding each parent node. That is, following the low-pass and high-pass filtering, when expanding a parent node, retain either all the odd samples or all the even samples, according to the choice which minimizes the cost function.

In this work, which is summarized in [8], we generate a *shifted wavelet packet* (SWP) library and introduce a *shift-invariant wavelet packet decomposition* (SIWPD) algorithm for a 'best basis' selection with respect to an additive cost function (e.g., entropy). We prove that the proposed algorithm leads to a best-basis representation that is both shift invariant and orthogonal. To demonstrate the shift-invariant properties of SIWPD, compared to WPD which lacks this feature, we refer to the expansions of the signals $g(t)$ (Fig. 2) and $g(t-2^{-6})$. These signals contain $2^7 = 128$ samples. For definiteness, we choose $D_8$ to serve as the scaling function ($D_8$ corresponds to 8-tap Daubechies minimum phase wavelet filters [17; 18, p. 198]) and entropy as the cost function. Figs. 3 and 4 depict the 'best-basis' expansion under the WPD and the SIWPD algorithms, respectively. A comparison of Figs. 3(b) and (d) readily reveals the sensitivity of WPD to temporal shifts while the

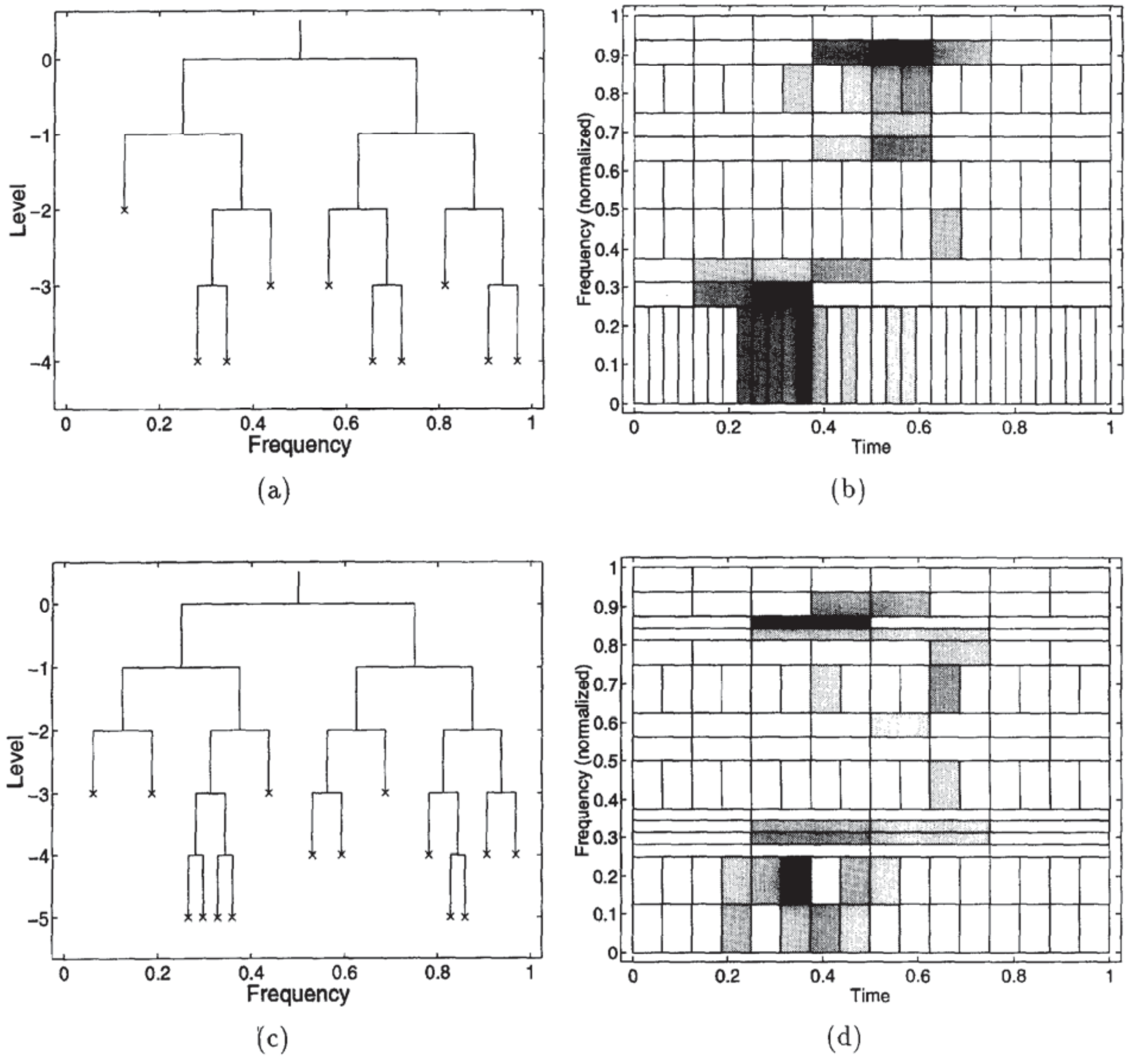


Fig. 3. Effects of a temporal shift on the time-frequency representation using the WPD with 8-tap Daubechies minimum phase wavelet filters: (a) the best expansion tree of $g(t)$, (b) $g(t)$ in its best basis; entropy = 2.84, (c) the best expansion tree of $g(t-2^{-6})$, (d) $g(t-2^{-6})$ in its best basis; entropy = 2.59.

best-basis SIWPD representation is indeed shift invariant and is characterized by a lower entropy (Fig. 4). It is worthwhile mentioning that the tiling grids in Figs. 3 and 4 do not in general correspond to actual time–frequency energy distributions. In fact, the energy distribution associated with each of the nominal rectangles may spread well beyond their designated areas [14]. However, when a proper 'scaling function' is selected (i.e., well localized in both time and frequency), the SIWPD based time-frequency representation resembles shift-invariant time-frequency distributions. Fig. 5 displays the Wigner and smoothed Wigner distributions [7] for the signal $g(t)$. The smoothing kernel (here we

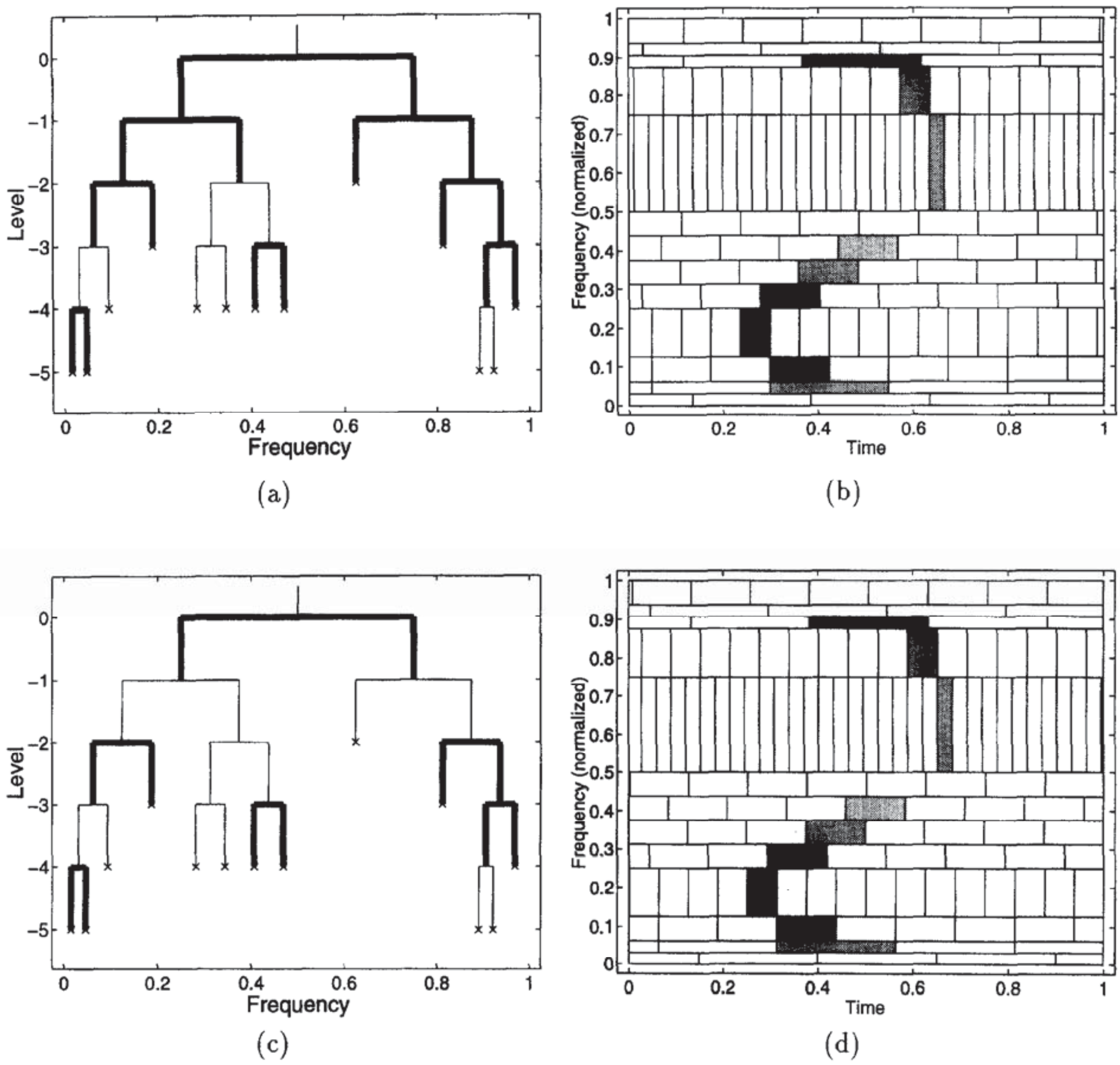


Fig. 4. Time–frequency representation using the SIWPD with 8-tap Daubechies minimum phase wavelet filters: (a) the best expansion tree of $g(t)$, (b) $g(t)$ in its best basis; entropy = 1.92, (c) the best expansion tree of $g(t-2^{-6})$, (d) $g(t-2^{-6})$ in its best basis; entropy = 1.92. Compared with the WPD (Fig. 3), beneficial properties are shift invariance and lower information cost.

chose a Gaussian) attenuates the interference terms at the expense of reduced time–frequency resolution. Obviously, the smoothed distribution (Fig. 5(b)) has a closer relation to the SIWPD based representation (Fig. 4(b)), than to the WPD based representation (Fig. 3(b)).

Pursuing the SIWPD algorithm, shift invariance is achieved by the introduction of an additional degree of freedom. The added dimension is a *relative shift* between a given parent node and its respective children nodes. Specifically, upon expanding a prescribed node, with minimization of the

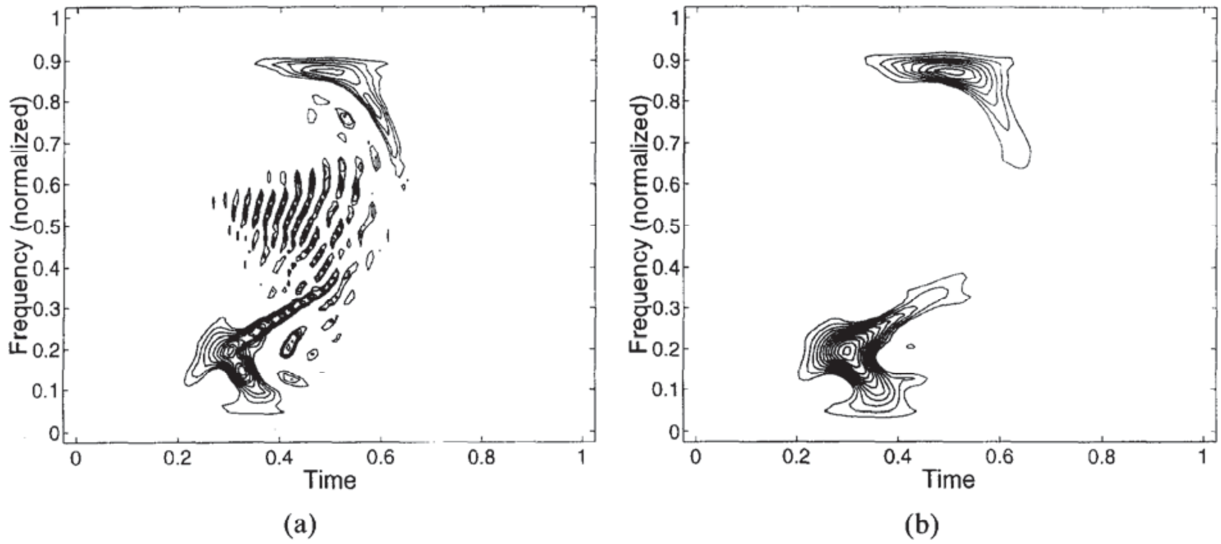


Fig. 5. Contour plots of time–frequency distributions for the signal $g(t)$: (a) Wigner distribution; (b) smoothed Wigner distribution. Notice the close relation between the smoothed Wigner distribution and the SIWPD based time–frequency representation which is depicted in Fig. 4(b).

information cost in mind, we test as to whether or not the information cost indeed decreases. We prove that for any given parent node it is sufficient to examine and select one of two alternative decompositions, made feasible by the SWP library. These decompositions correspond to a zero shift and a $2^{-\ell}$ shift where $\ell$ $(-L \leqslant \ell \leqslant 0)$ denotes the resolution level. The special case where, at any resolution level, only low frequency nodes are further expanded corresponds to a *shift-invariant wavelet transform* (SIWT) [30, 36]. An alternative view of SIWPD is facilitated via filter-bank terminology [40, 44]. Accordingly, each parent node is expanded by high-pass and low-pass filters, followed by a 2 : 1 down sampling. In executing WPD, down sampling is achieved by ignoring all even-indexed (or all odd-indexed) terms. In contrast, when pursuing SIWPD, the down sampling is carried out *adaptively* for the prescribed signal. We stress that owing to the orthogonality of the representation and the presumed additive nature of the cost function (e.g., entropy or rate distortion), the decision at any given node is strictly local, i.e., independent of other notes at the same resolution level.

The SIWPD expansion generates an ordinary binary tree [15]. However, each generated branch

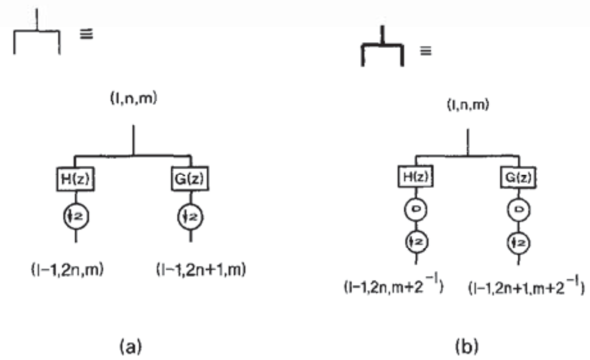


Fig. 6. A 'parent' node binary expansion according to SIWPD: (a) high- and low-pass filtering followed by a 2 : 1 downsampling, (b) high- and low-pass filtering followed by a one sample delay ($D$) and subsequently by a 2 : 1 downsampling.

is now designated by either fine or heavy lines (Fig. 6) depending on the adaptive selection of the odd or the even terms, respectively. It can be readily observed that in contrast to WPD, SIWPD expansion leads to tree configurations that are independent of the time origin. Fine and heavy lines may, however, exchange positions (e.g., compare Figs. 4(a) and (c)).

The computational complexity of executing a best-basis SIWPD expansion is $O[2^d(L-d+2)N]$, where $N$ denotes the length of the signal (at its highest resolution level), $L+1$ is the number of resolution levels ($L \leqslant \log_2 N$) and $d$ is the maximum depth of a subtree used at a given parent-node to determine the shift mode of its children ($1 \leqslant d \leqslant L$). In the extreme case $d=1$, the complexity, $O(NL)$, is similar to that associated with WPD, and the representation merges with that proposed in [22]. As a rule, the larger $d$ and $L$, the larger the complexity, however, the determined best basis is of a higher quality; namely, characterized by a lower information cost.

For $d=L$ and for an identical number of resolution levels, SIWPD leads necessarily to an information cost that is lower than or equal to that resulting from standard WPD. This observation stems directly from the fact that WP library constitutes a subset of the SWP library. In other words, WPD may be viewed as a degenerate form of SIWPD characterized by $d=0$. In this case, the relative shift of newly generated nodes is non-adaptively set to zero and generally leads to shift-variant representations.

The best-basis expansion under SIWPD is also characterized by the invariance of the information cost. This feature is significant as it facilitates a meaningful quantitative comparison between alternative SWP libraries. Usually such a comparison between alternative libraries lacks meaning for WP, as demonstrated by the example summarized in Table 1.

Table 1
Entropies of $g(t)$ (Fig. 2) and $g(t-2^{-6})$ represented on 'best bases' obtained via WPD and SIWPD using libraries derived from $D_8$ and $C_6$ scaling functions

| | WPD | | SIWPD | |
|---|---|---|---|---|
| | $D_8$ | $C_6$ | $D_8$ | $C_6$ |
| $g(t)$ | 2.84 | **2.75** | **1.92** | 2.35 |
| $g(t-2^{-6})$ | **2.59** | 2.69 | **1.92** | 2.35 |

Note: $D_8$ corresponds to 8-tap Daubechies wavelet filters, and $C_6$ corresponds to 6-tap coiflet filters.

Here, the entropies of the signals $g(t)$ (Fig. 2) and $g(t-2^{-6})$ are compared. The expansions are on the best bases stemming from both the WPD and SIWPD algorithms and for $D_8$ and $C_6$ scaling functions ($C_6$ corresponds to 6-tap coiflet filters [18, p. 261; 19]). We can readily observe the shift-invariance under SIWPD and the fact that the selection of $D_8$ is consistently advantageous over $C_6$. Just as obvious is the futility of attempting a comparison between the $C_6$ and $D_8$ based libraries under WPD. $C_6$ is better for $g(t)$ while $D_8$ is advantageous in representing $g(t-2^{-6})$.

This paper is structured as follows. In Section 2, we introduce a shifted wavelet packet library as a collection of orthonormal bases. Section 3 describes a best-basis selection algorithm. It is proved that the resultant best basis decomposition and the corresponding expansion tree are indeed shift invariant. A shift-invariant wavelet transform is described in Section 4. The trade-off between computational complexity and information cost is the subject matter of Section 5, while Section 6 briefly discusses the important extension to two-dimensional signals.

## 2. The shifted wavelet packet library

Let $\{h_n\}$ denote a real-valued quadrature mirror filter (QMF) obeying (e.g., [17, Theorem 3.6, p. 964]

$$\sum_n h_{n-2k} h_{n-2\ell} = \delta_{k,\ell}, \tag{1}$$

$$\sum_n h_n = \sqrt{2}. \tag{2}$$

Let $\{\psi_n(x)\}$ be a wavelet packet family (e.g., [13, 49]) defined and generated via

$$\psi_{2n} = \sqrt{2}\sum_k h_k \psi_n(2x-k), \tag{3}$$

$$\psi_{2n+1}(x) = \sqrt{2}\sum_k g_k \psi_n(2x-k), \tag{4}$$

where $g_k = (-1)^k h_{1-k}$, and $\psi_0(x) \equiv \varphi(x)$ is an orthonormal scaling function, satisfying

$$\langle \varphi(x-p), \varphi(x-q)\rangle = \delta_{p,q}, \quad p, q \in \mathbb{Z}. \tag{5}$$

Furthermore, let $f(x)$ be a function specified at the $j$th resolution level, i.e., $f \in V_j$, where

$$V_j = \operatorname{clos}_{L^2(\mathbb{R})}\{2^{j/2}\psi_0(2^j x - k)\colon k \in \mathbb{Z}\}. \tag{6}$$

It may be observed that the expansion of $f(x)$ on the standard basis $\{2^{j/2}\psi_0(2^j x - k)\colon k \in \mathbb{Z}\}$ remains invariant under $2^{-j}m$ shifts ($m \in \mathbb{Z}$). However, as $f(x) \in V_j$ is decomposed into orthonormal wavelet packets using the best-basis algorithm of Coifman and Wickerhauser [15], the often crucial property of shift invariance is no longer valid. One way to achieve shift invariance is to adjust the time localization of the basis functions [8, 30, 37]. That is, when an analyzed signal is translated in time by $\tau$, a new best basis is selected whose elements are also translated by $\tau$ compared to the former best basis. Consequently, the expansion coefficients, that are now associated with translated basis functions, stay unchanged and the time–frequency representation is shifted in time by the same period. The ordinary construction of a wavelet packet (WP) library precludes the above procedure, since translated versions of library bases are not necessarily included in the library. The proposed strategy in obtaining shift invariance is based on extending the library to include all their shifted versions, organizing it in a tree structure and providing an efficient 'best basis' search algorithm.

To further pursue the stated objective we introduce the notation [8, 37]

$$B^j_{\ell,n,m} = \{2^{(\ell+j)/2}\psi_n[2^\ell(2^j x - m) - k]\colon k \in \mathbb{Z}\}, \tag{7}$$

$$U^j_{\ell,n,m} = \operatorname{clos}_{L^2(\mathbb{R})}\{B^j_{\ell,n,m}\} \tag{8}$$

and define *shifted-wavelet-packet* (SWP) library as a collection of all the orthonormal bases for $V_j$ which are subsets of

$$\{B^j_{\ell,n,m}\colon \ell \in \mathbb{Z}_-,\ n \in \mathbb{Z}_+,\ 0 \leqslant m < 2^{-\ell}\}. \tag{9}$$

This library is larger than the WP library by a square power, but it can still be cast into a tree configuration facilitating fast search algorithms. The tree structure is depicted in Fig. 7(a). Each node in the tree is indexed by the triplet $(\ell, n, m)$ and represents the subspace $U^j_{\ell,n,m}$. Likewise the ordinary binary trees [15], the nodes are identified with dyadic intervals of the form $I_{\ell,n} = [2^\ell n, 2^\ell(n+1))$. The additional parameter $m$ provides degree of freedom to adjust the time-localization of the basis functions. The following proposition gives simple graphic conditions on subsets forming orthonormal bases.

**Proposition 1** [8]. *Let $E = \{(\ell, n, m)\} \subset \mathbb{Z}_- \times \mathbb{Z}_+ \times \mathbb{Z}_+$, $0 \leqslant m < 2^{-\ell}$, denote a collection of indices satisfying*
(i) *The segments $I_{\ell,n} = [2^\ell n, 2^\ell(n+1))$ are a disjoint cover of $[0,1)$.*
(ii) *The shift indices of a pair of nodes $(\ell_1, n_1, m_1)$, $(\ell_2, n_2, m_2) \in E$ are related by*

$$m_1 \bmod 2^{-\hat{\ell}+1} = m_2 \bmod 2^{-\hat{\ell}+1}, \tag{10}$$

*where $\hat{\ell}$ is the level index of a dyadic interval $I_{\hat{\ell},\hat{n}}$ that contains both $I_{\ell_1,n_1}$ and $I_{\ell_2,n_2}$.*
*Then $E$ generates an orthonormal (ON) basis for $V_j \equiv U^j_{0,0,0}$, i.e., $\{B^j_{\ell,n,m}\colon (\ell,n,m) \in E\}$ is an ON basis, and the set of all $E$ as specified above generates an SWP library.*

Condition (ii) is equivalent to demanding that the relative shift between a prescribed parent node $(\ell, n, m)$ and all its children nodes is necessarily a constant whose value is restricted to either zero or to $2^{-\ell}$. In the dyadic one-dimensional case, each parent node $(\ell, n, m)$ generates children nodes $(\ell - 1, 2n, m')$ and $(\ell - 1, 2n+1, m'')$ where, according to condition (ii), their shift indices may take the value $m' = m'' = m$ or $m' = m'' = m + 2^{-\ell}$ (the generated branches are respectively depicted by thin or heavy lines; cf. Fig. 6).

The expansion tree associated with a given signal describes the signal's representation on an orthonormal basis selected from the SWP library. The index set $E$ is interpreted as the collection of all terminal nodes. That is, all nodes beyond which no further expansion is to be carried out. A specific example of an expansion tree is shown in Fig. 7(b). The proposed configuration ensures that the set of terminal nodes satisfies the conditions of Proposition 1. In particular, refer to the terminal nodes $(-3, 0, 6)$ and $(-4, 5, 10)$. These nodes are descendants of $(-1, 0, 0)$. Hence, their related dyadic intervals $I_{-3,0} = [0, 1/8)$ and $I_{-4,5} = [5/16, 3/8)$ are contained in the dyadic interval $I_{-1,0} = [0, 1/2)$, and their shift indices are indeed related by

$$6 \bmod 2^2 = 10 \bmod 2^2 = 2.$$

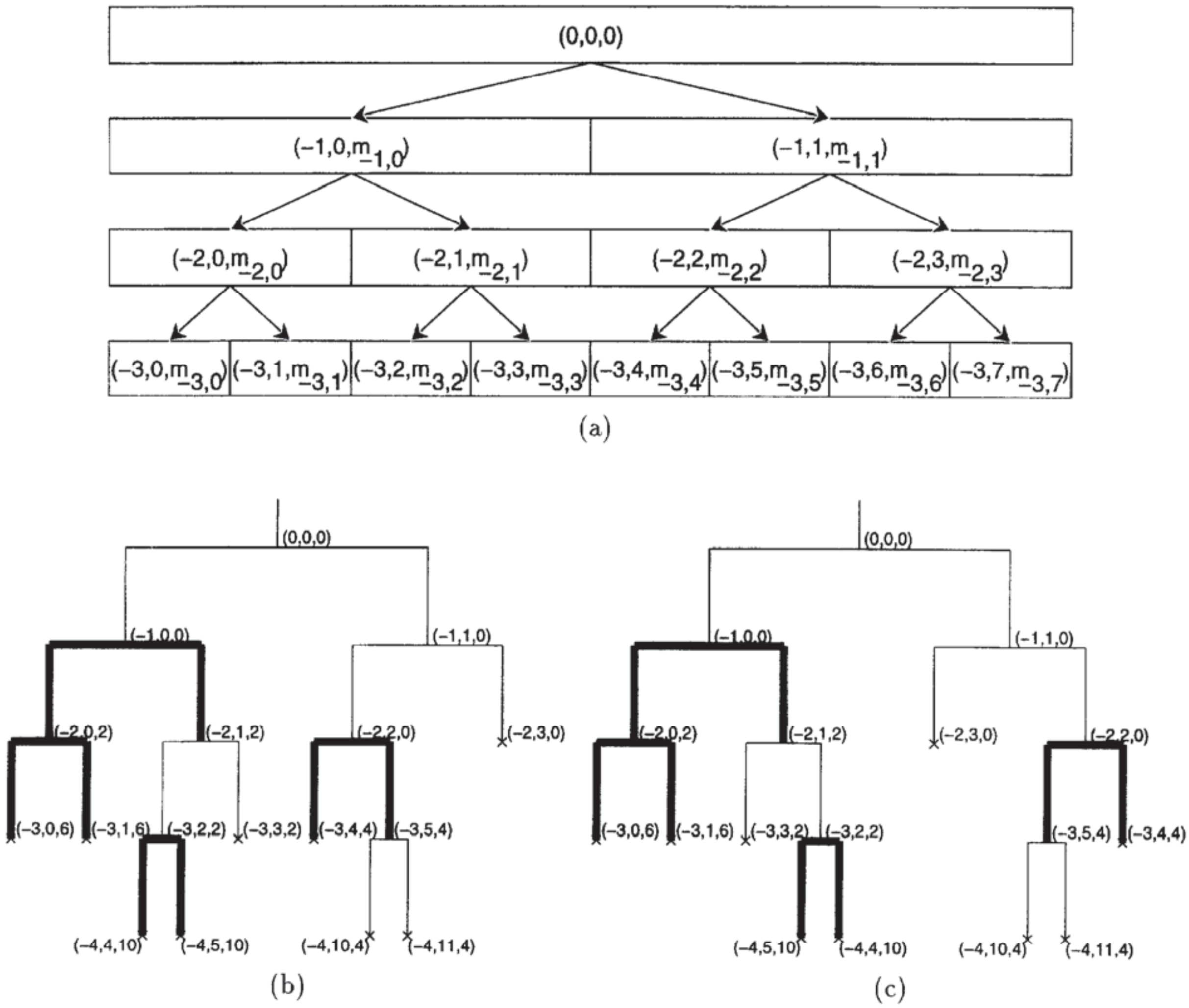

Fig. 7. (a) The extended set of wavelet packets organized in a binary tree structure. Each node in the tree is indexed by the triplet $(\ell, n, m)$ and represents the subspace $U^j_{\ell,n,m}$. (b) Exemplifying an SIWPD binary tree. The children nodes corresponding to $(\ell, n, m)$ are $(\ell-1, 2n, \tilde{m})$ and $(\ell-1, 2n+1, \tilde{m})$, where $\tilde{m} = m$ (depicted by thin lines) or $\tilde{m} = m + 2^{-\ell}$ (depicted by heavy lines). (c) Rearrangement of the nodes in a *sequence order*.

The nodes of each level in this example have a natural or *Paley* order. It is normally useful to rearrange them in a *sequency* order [49], so that the nominal frequency of the associated wavelet packets increases as we move from left to right along a level of the tree. The rule to get a sequency ordered tree is to exchange the two children nodes of each parent node with odd sequency (inverse Gray code permutation [49, p. 250]). The resultant tree is depicted in Fig. 7(c).

## 3. The best basis selection

Alike the wavelet packet library [15], the tree configuration of the extended library facilitates an efficient best basis selection process. However, in contrast to the WPD, the best basis representation is now shift invariant.

Let $f \in V_j = U^j_{0,0,0}$, let $\mathscr{M}$ denote an additive cost function and let $\mathscr{B}$ represent an SWP library.

**Definition 1** [15]. The best basis for $f$ in $\mathscr{B}$ with respect to $\mathscr{M}$ is $B \in \mathscr{B}$ for which $\mathscr{M}(Bf)$ is minimal. Here, $\mathscr{M}(Bf)$ is the information cost of representing $f$ in the basis $B \in \mathscr{B}$.

Let $A^j_{\ell,n,m}$ denote the best basis for the subspace $U^j_{\ell,n,m}$. Accordingly, $A^j_{0,0,0}$ constitutes the best basis for $f \in V_j$ with respect to $\mathscr{M}$. Henceforth, for notational simplicity, we omit the fixed index $j$. The desired best basis can be determined recursively by setting

$$A_{\ell,n,m} = \begin{cases} B_{\ell,n,m} & \text{if } \mathscr{M}(B_{\ell,n,m}f) \leqslant \mathscr{M}(A_{\ell-1,2n,m_c}f) \\ & \quad + \mathscr{M}(A_{\ell-1,2n+1,m_c}f), \\ A_{\ell-1,2n,m_c} \oplus A_{\ell-1,2n+1,m_c}, & \text{else}, \end{cases} \tag{11}$$

where the shift indices of the respective children nodes are given by

$$m_c = \begin{cases} m, & \text{if } \sum_{i=0}^{1} \mathscr{M}(A_{\ell-1,2n+i,m}f) \\ & \quad \leqslant \sum_{i=0}^{1} \mathscr{M}(A_{\ell-1,2n+i,m+2^{-\ell}}f), \\ m + 2^{-\ell}, & \text{else}. \end{cases} \tag{12}$$

The recursive sequence proceeds down to a specified level $\ell = -L$ ($L \leqslant \log_2 N$), where

$$A_{-L,n,m} = B_{-L,n,m}. \tag{13}$$

The stated procedure resembles that proposed by Coifman and Wickerhauser [15] with an added degree of freedom facilitating a relative shift (i.e., $m_c \neq m$) between a parent node and its respective children nodes. It is re-emphasized that the recursion considered herein restricts the shift to one of two values ($m_c - m \in \{0, 2^{-\ell}\}$). Other values are unacceptable if the orthonormality of the best basis is to be preserved. As it turns out, the generated degree of freedom is crucial in establishing time invariance. The recursive sequence proposed in [15] may be viewed as a special case where $m_c - m$ is arbitrarily set to zero.

**Lemma 1.** *Let $E_1$ and $E_2$ denote index collections obeying Proposition 1, and let $B_1$ and $B_2$ be the corresponding orthonormal bases. Then $B_1$ and $B_2$ are 'identical to within a time-shift' if and only if there exists a constant $q \in \mathbb{Z}$ such that for all $(\ell, n, m) \in E_1$, we have $(\ell, n, \tilde{m}) \subset E_2$ where $\tilde{m} = (m + q) \bmod 2^{-\ell}$.*

**Proof.** Bases in $V_j$ are said to be *identical to within a time shift* if and only if there exists $q \in \mathbb{Z}$ such that for each element in $B_1$ we have an identical element in $B_2$ that is time shifted by $q2^{-j}$. Namely, if

$$2^{(\ell+j)/2}\psi_n[2^\ell(2^j x - m) - k] \in B_1,$$

then

$$2^{(\ell+j)/2}\psi_n[2^\ell(2^j(x - q2^{-j}) - m) - k] \in B_2,$$

If $E$ denotes index collection obeying Proposition 1 and $B$ is its corresponding basis, then $(\ell, n, m) \in E$ is equivalent to $B^j_{\ell,n,m} \subset B$. Therefore, by observing that

$$\psi_n[2^\ell(2^j(x - q2^{-j}) - m) - k] \\ = \psi_n[2^\ell(2^j x - \tilde{m}) - \tilde{k}],$$

where $\tilde{m} = (m + q) \bmod 2^{-\ell}$ and $\tilde{k} = k + \lfloor 2^\ell(m + q) \rfloor$, the proof is concluded. □.

**Definition 2.** Binary trees are said to be 'identical to within a time shift' if they correspond to bases that are 'identical to within a time shift'.

Figs. 4(a) and (c) depict *identical to within a time shift* trees representing the identical to within time-shift signals.

**Proposition 2.** *The best basis expansion stemming from the previously described recursive algorithm is shift invariant.*

**Proof.** Let $f$, $g \in V_j$ be identical to within a time shift, i.e., there exists $q \in \mathbb{Z}$ such that $g(x) = f(x - q2^{-j})$. Let $A_f$ and $A_g$ denote the best bases for $f$ and $g$, respectively. It can be shown (Appendix A) that

$$B_{\ell,n,m} \subset A_f$$

implies

$$B_{\ell,n,\tilde{m}} \subset A_g, \quad \tilde{m} = (m + q) \bmod (2^{-\ell}),$$

for all $m, n \in \mathbb{Z}_+$ and $\ell \in \mathbb{Z}_-$. Hence, $A_f$ and $A_g$ are *identical to within a time shift.* □

The number of orthonormal bases contained in the shifted WP library can be computed recursively. Let $S_L$ denote the number of bases associated with an $(L+1)$-level tree expansion (i.e., the expansion is to be executed down to the $\ell = -L$ level). The tree comprises a root and two $L$-level subtrees. Since two options exist for selecting the relative shift, we have

$$S_L = 1 + 2S_{L-1}^2, \quad S_0 = 1. \tag{14}$$

Consequently, it can be shown by induction that for $L > 2$

$$0.5(2.48)^{2^L} < S_L < 0.5(2.49)^{2^L}. \tag{15}$$

A length $N$ signal may be represented by $S_L$ different orthonormal bases ($L \leqslant \log_2 N$), from which the best basis is selected. While the associated complexity level is of $O(N2^{L+1})$, we demonstrate in Section 5 that the algorithmic complexity may be reduced substantially (down to a level of $O(NL)$) while still retaining shift invariance. The reduced complexity, however, may lead to representations characterized by a higher cost function values.

For the sake of comparison with the established WPD algorithm [15], let $s_L$ denote the number of bases associated with an $(L+1)$-level tree. Then

$$s_L = 1 + s_{L-1}^2, \quad s_0 = 1, \tag{16}$$

and consequently, for $L > 2$

$$(1.50)^{2^L} < s_L < (1.51)^{2^L}. \tag{17}$$

The WPD algorithm has an attractive complexity level of $O(NL)$. However, the best basis representation is not shift invariant. It is worthwhile stressing that despite the fact that $S_L > s_L^2$ for $L > 2$, the complexity level characterizing SIWPD is significantly below the squared WPD complexity. Specifically, $O(N2^{L+1}) \ll O(N^2L^2)$.

## 4. The shift-invariant wavelet transforms

The property of shift invariance can also be achieved within the framework of the wavelet transform (WT) and a prescribed information cost function ($\mathscr{M}$) [30, 36]. It may be viewed as a special case whereby the tree configuration is constrained to expanding exclusively the *low-frequency* nodes. The signal is expanded by introducing a scaling function ($\psi_0$) or a 'mother wavelet' ($\psi_1$). To achieve shift invariance, we again permit the introduction of a relative shift between children nodes and their parent node. The shift selection is, once again, based on minimizing the cost function ($\mathscr{M}$) at hand. This procedure yields the *wavelet best basis* for a signal $f \in V_j$ with respect to ($\mathscr{M}$), among all the orthonormal bases generated by

$$\{B_{\ell,n,m}^j : \ell \in \mathbb{Z}_-, n \in (0,1), 0 \leqslant m < 2^{-\ell}\}.$$

Let $W_{\ell,m}$ denote the *wavelet best basis* for $U_{\ell,0,m}^j$. The *wavelet best basis* for $f \in V_j \equiv U_{0,0,0}^j$ may be determined recursively via

$$W_{\ell,m} = W_{\ell-1,m_c} \oplus B_{\ell-1,1,m_c}^j, \tag{18}$$

where

$$m_c = \begin{cases} m, & \text{if } \mathscr{M}(W_{\ell-1,m}f) + \mathscr{M}(B_{\ell-1,1,m}^j f) \\ & \quad \leqslant \mathscr{M}(W_{\ell-1,m+2^{-\ell}}f) \\ & \quad + \mathscr{M}(B_{\ell-1,1,m+2^{-\ell}}^j f). \\ m + 2^{-\ell}, & \text{else}. \end{cases} \tag{19}$$

The expansion is performed down to the level $\ell = -L$ ($L \leqslant \log_2 N$), namely

$$W_{-L,m} = B_{-L,0,m}^j. \tag{20}$$

An $N$-element signal may be represented by $2^L$ different orthonormal wavelet bases. The associated complexity level is $O(NL)$ and the resultant expansion is indeed shift invariant.

As an example, we now refer to the signal $g(t)$, depicted in Fig. 2, and its translation $g(t-2^{-6})$. The corresponding wavelet transforms, with $C_6$ as the scaling function [18, p. 261; 19], are described in Fig. 8. The variations in the energy spreads of $g(t)$ and $g(t-2^{-6})$, stemming directly from the lack of shift invariance, are self-evident. Moreover, the transformed cost function (entropy) is shift dependent as well. In complete contrast, the *wavelet best basis* decompositions depicted in Fig. 9 yield identical (to within a time shift) energy distributions. The corresponding entropy is lower and independent of the time shift.

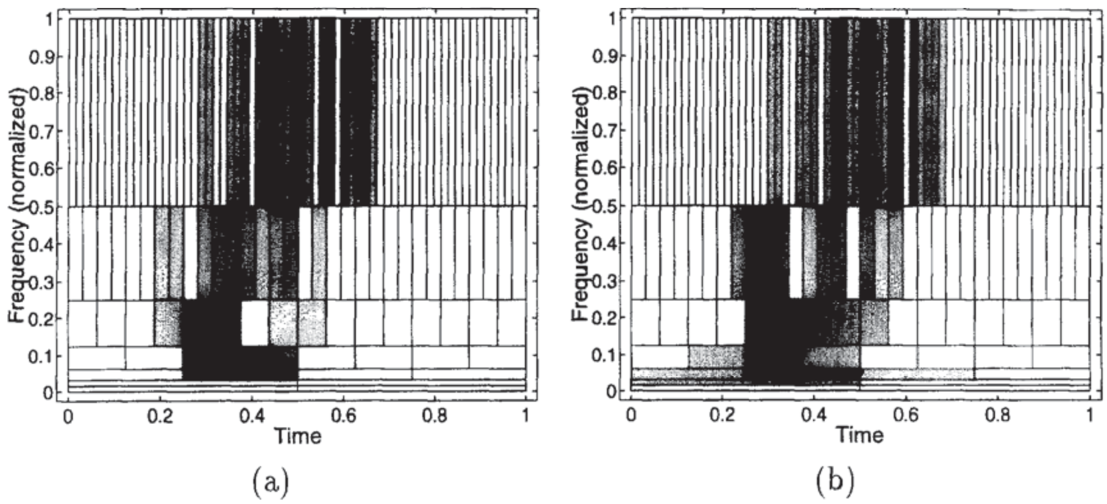


Fig. 8. Time–frequency representation in the wavelet basis using 6-tap coiflet filters: (a) the signal $g(t)$; entropy = 3.22; (b) the signal $g(t-2^{-6})$; entropy = 3.34.

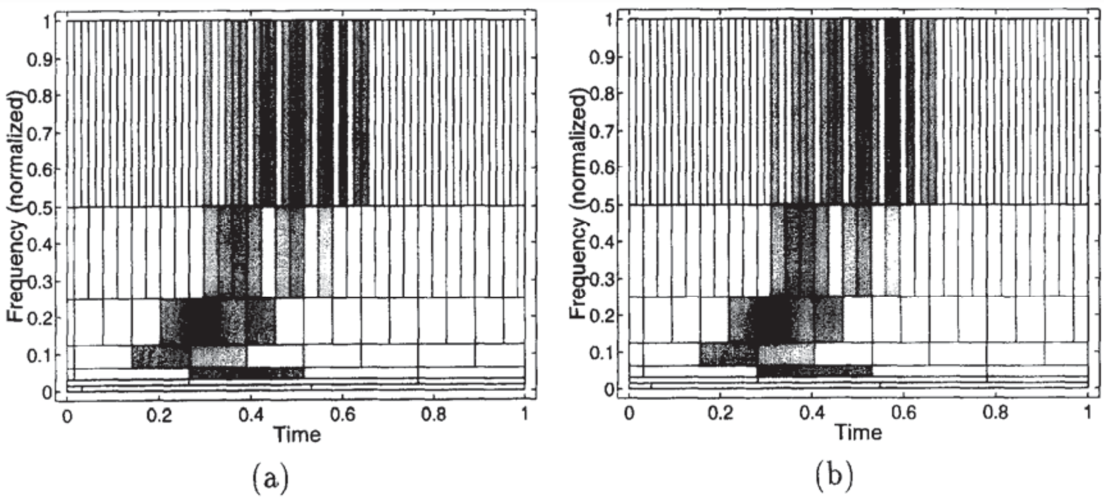


Fig. 9. Time–frequency representation in the wavelet best basis using 6-tap coiflet filters: (a) the signal $g(t)$; entropy = 3.02; (b) the signal $g(t-2^{-6})$; entropy = 3.02.

## 5. The information-cost complexity trade-off

So far we have observed that WPD lacks shift invariance but is characterized by an attractive complexity level $O(NL)$, where $L$ denotes the lowest resolution level in the expansion tree. Comparatively, the quadratic complexity level, $O(N2^{L+1})$, associated with SIWPD is substantially higher. In return, one may achieve a potentially large reduction of the information cost, in addition to gaining the all important *shift invariance*. However, whenever the SIWPD complexity is viewed as intolerable, one may resort to a suboptimal SIWPD procedure entailing a reduced complexity, and higher information cost while still retaining the desirable shift invariance.

The best basis for $f \in V_j$ with respect to $\mathscr{M}$ is, once again, obtained recursively via (11), but contrary to the procedure of Section 3, now the selection of a relative shift at a given parent node does not necessitate tree expansion down to the lowest level. While an optimal decision on the value of a shift index is provided by (12), a suboptimal shift index may be determined by

$$m_c = \begin{cases} m & \text{if } \sum_{i=0}^{1} \mathscr{M}(C_{\ell-1,2n+i,m,d}f) \\ & \quad \leqslant \sum_{i=0}^{1} \mathscr{M}(C_{\ell-1,2n+i,m+2^{-\ell},d}f), \\ m+2, & \text{else}, \end{cases} \tag{21}$$

where $C_{\ell,n,m,d}$ denotes the best basis for $U_{\ell,n,m}$ subject to constraining the decomposition to $d$ $(1 \leqslant d \leqslant L)$ resolution levels. Accordingly, the shift indices are estimated using subtrees of $d_\ell$ resolution levels depth $(d_\ell \leqslant d)$, where

$$d_\ell = \begin{cases} d, & d - L \leqslant \ell \leqslant 0, \\ L + \ell, & \text{else}. \end{cases} \tag{22}$$

For $d = 1$ or at the coarsest resolution level $\ell = -L$ we have $C_{\ell,n,m,d} = B_{\ell,n,m}$. For $\ell > -L$ and $d > 1$ $C_{\ell,n,m,d}$ is obtained recursively according to

$$C_{\ell,n,m,d} = \begin{cases} B_{\ell,n,m}, \\ C_{\ell-1,2n,m,d-1} \oplus C_{\ell-1,2n+1,m,d-1}, \\ C_{\ell-1,2n,m+2^{-\ell},d-1} \oplus C_{\ell-1,2n+1,m+2^{-\ell},d-1}, \end{cases} \tag{23}$$

where $C_{\ell,n,m,d}$ takes on that value which minimizes the cost function $\mathscr{M}$.

The shift invariance is retained for all $1 \leqslant d \leqslant L$. The cases $d = L$ and $d < L$ should be viewed as *optimal* and *suboptimal* with respect to the prescribed information cost function ($\mathscr{M}$). The best-basis search algorithm of Coifman and Wickerhauser [15] corresponds to the special case $m_c = m$ for all nodes ($d \equiv 0$). Quite expectedly, the non-adaptive selection yields representations that are not, in general, shift invariant. Fig. 10 depicts the time-frequency representations of the signals $g(t)$ and $g(t - 2^{-6})$, using the suboptimal SIWPD($d = 1$) with 8-tap Daubechies minimum phase wavelet filters. The resultant entropy is higher

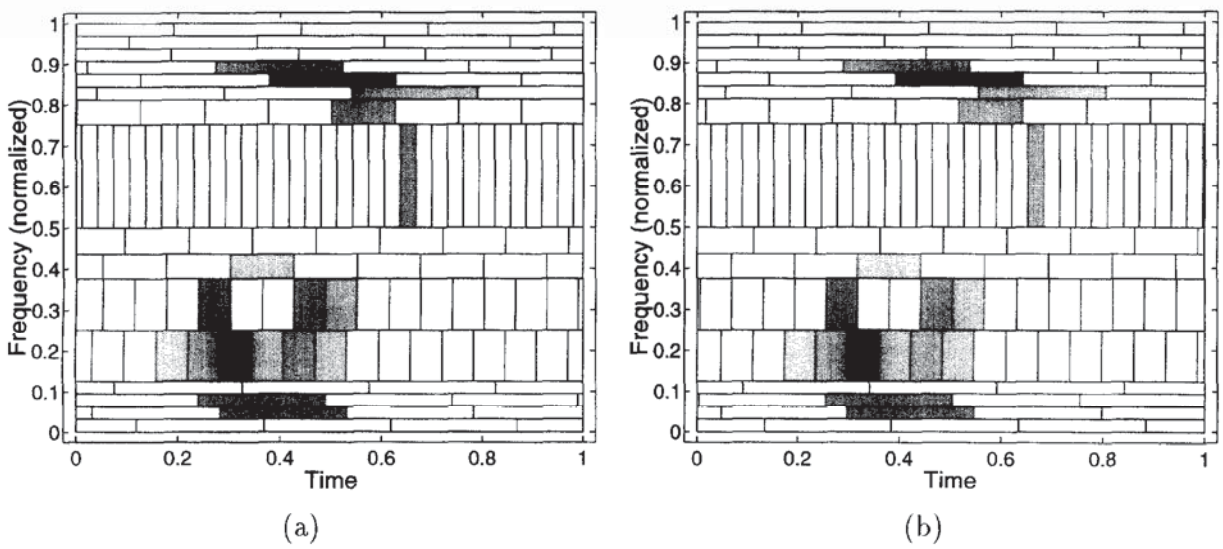


Fig. 10. Time-frequency representation using the suboptimal ($d = 1$) SIWPD with 8-tap Daubechies minimum phase wavelet filters: (a) the signal $g(t)$; entropy = 2.32; (b) the signal $g(t - 2^{-6})$; entropy = 2.32.

than is obtained using the optimal SIWPD (Fig. 4). Yet, the valuable property of shift invariance is provided with a significant reduction in the computational complexity.

Since, at each level $\ell$, the subtrees employed in estimating the shift indices are restricted to $d_\ell$ level depth ($d_\ell \leqslant d$), the complexity is now $\mathrm{O}[N2^d(L-d+2)]$. In the extreme case, $d=1$, the complexity, $\mathrm{O}(2NL)$, resembles that associated with WPD, and the representation merges with that proposed in [22]. As a rule, the larger $d$ and $L$, the larger the complexity, however, the determined best basis is of a higher quality; namely, characterized by a lower information cost.

### *5.1. Example*

To demonstrate the trade-off between information cost and complexity we refer to Figs. 11–13. These figures depict the expansion trees of the signal $g(t)$, either when the relative shifts are arbitrarily set to zero (the WPD algorithm), estimated using one-level-depth subtrees (suboptimal SIWPD with $d=1$), or estimated using two-levels-depth subtrees (suboptimal SIWPD with $d=2$). The numbers associated with the nodes of the tree represent the entropies of $g$ in the corresponding subspaces. For the best expansion trees, the numbers represent the minimum entropies obtained by the best-basis algorithms.

The initial entropy of the signal $g$ is 3.58. The children nodes of the root node have lower entropy when we introduce a relative shift (regarding Figs. 11(a) and 12(a): $1.85 + 1.41 < 1.84 + 1.48$). Hence the root-node decomposition in Fig. 12(a) is carried out with 'heavy lines'. Now, consider the expansion of the node specified by $(\ell, n, m) = (-1, 0, 1)$ (the left node at the level $\ell = -1$). If the relative shift is

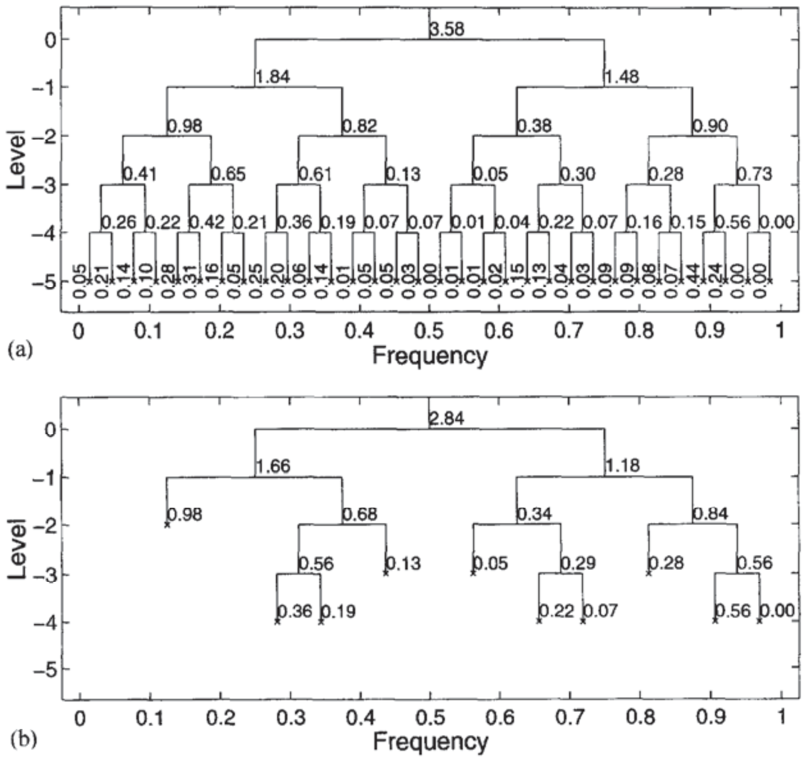


Fig. 11. Wavelet packet library trees of the signal $g(t)$: (a) five-level expansion tree; the numbers represent the entropies of $g$ in the corresponding subspaces; (b) the best expansion tree; the numbers represent the minimum entropies obtained by the best-basis algorithm.

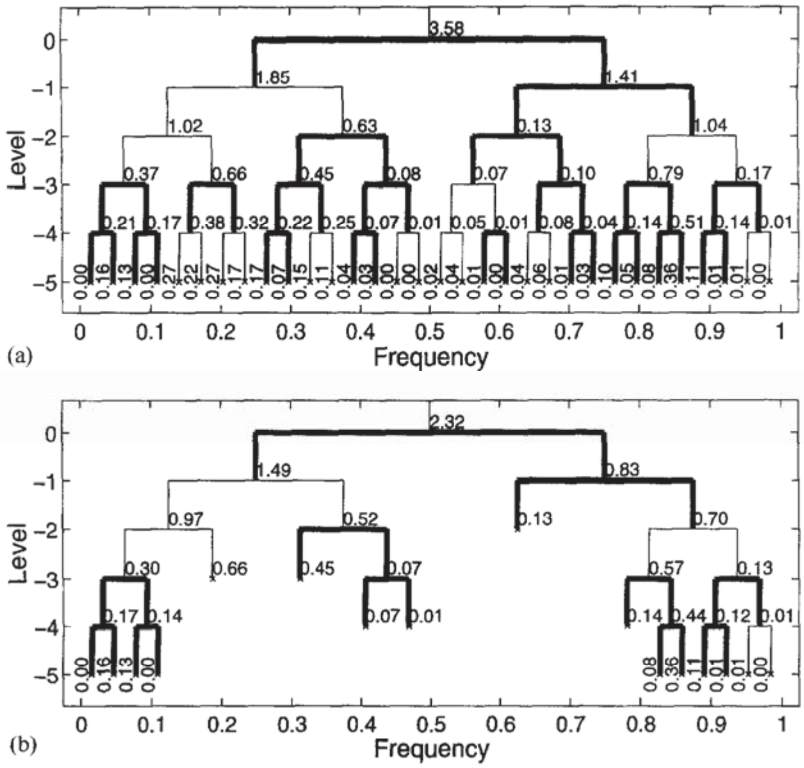

Fig. 12. Shifted wavelet packet library trees of the signal $g(t)$: (a) five-level expansion tree, where the relative shifts are estimated using one-level-depth subtrees ($d = 1$), the numbers represent the entropies of $g$ in the corresponding subspaces; (b) the best expansion tree, the numbers represent the minimum entropies obtained by the suboptimal ($d = 1$) best-basis algorithm.

based on a one-level-depth subtree, then no relative shift is required (regarding Figs 12(a) and 13(a): $1.02 + 0.63 < 1.09 + 0.70$). However, a deeper subtree reveals that a relative shift is actually more desirable, and a lower entropy for the node $(-1, 0, 1)$ is attainable (regarding Figs 12(b) and 13(b): $1.23 < 1.49$). The eventual entropy of the signal $g$ is 2.84 when implementing the WPD algorithm, 2.32 when using the suboptimal SIWPD($d = 1$), and 1.92 when using the suboptimal SIWPD($d = 2$). The number of real multiplications required by these algorithms are respectively $rNL = 5120$, $2rNL = 10\,240$ or $rN(4L - 2) = 18\,432$, where the length of the signal is $N = 128$, the number of decomposition levels is $L = 5$, and the filters' length is $r = 8$. In this particular example, larger $d$ values do not yield a further reduction in the information cost, since $d = 2$ has already reached the optimal SIWPD (compare Figs. 13(b) and 4(a)).

### 5.2. Experiment

Normally, as was the case for the above example, the information cost decreases when the shift indices are evaluated based on deeper subtrees (larger $d$). Notwithstanding an assured reduction in information cost using the optimal SIWPD, suboptimal SIWPD may anomalously induce an increase. We have performed an experiment on 50 acoustic transients, generated by explosive charges at various distances (these signals are detected by an array of receivers and used to evaluate the location of explosive devices). Fig. 14 shows a typical acoustic pressure waveform containing 64 samples. We

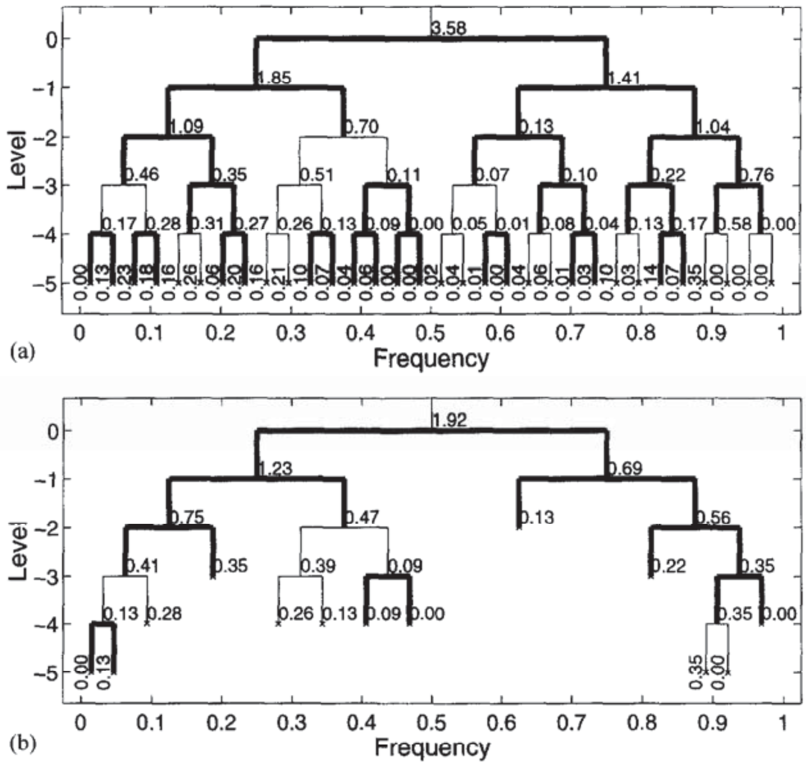


Fig. 13. Shifted wavelet packet library trees of the signal $g(t)$: (a) five-level expansion tree, where the relative shifts are estimated using two-levels-depth subtrees ($d = 2$), the numbers represent the entropies of $g$ in the corresponding subspaces; (b) the best expansion tree, the numbers represent the minimum entropies obtained by the suboptimal ($d = 2$) best-basis algorithm.

applied the WPD algorithm, the suboptimal SIWPD with $d = 1$ or $d = 2$, and the optimal SIWPD to the compression of this data set. The decomposition was carried out to maximum level $L = 5$ using 8-tap Daubechies minimum phase wavelet filters. The number of real multiplications required by these algorithms for expanding a given waveform in its best basis are respectively 2560, 5120, 9216 and 31744.

Table 2 lists the attained entropies by the best-basis algorithms for an arbitrary subset of ten waveforms. Clearly, the average entropy is lower when using the SIWPD. It decreases when $d$ is larger, and a minimum value is reached using the optimal SIWPD($d = L$). Moreover, the variations in the information cost, which indicate performance robustness across the data set, are also lower when using the SIWPD. Notice the irregularity pertaining to the eighth waveform. While its minimum entropy is expectedly obtained by implementing the optimal SIWPD, the suboptimal SIWPD with $d = 1$ fails to reduce the entropy in comparison with the conventional WPD.

To illustrate the improvement in information cost of the SIWPD with various $d$ values over the conventional WPD, we plot in Fig. 15 the reduction in entropy relative to the entropy obtained using the WPD. We can see that for some signals the entropy is reduced by more than 30%. The average reduction is 10.8% by the suboptimal SIWPD($d = 1$), 16.4% by the suboptimal SIWPD($d = 2$), and 18.1% by the optimal SIWPD. Thus the average performance of SIWPD is increasingly improved as we deepen the subtrees used in estimating the shift indices.

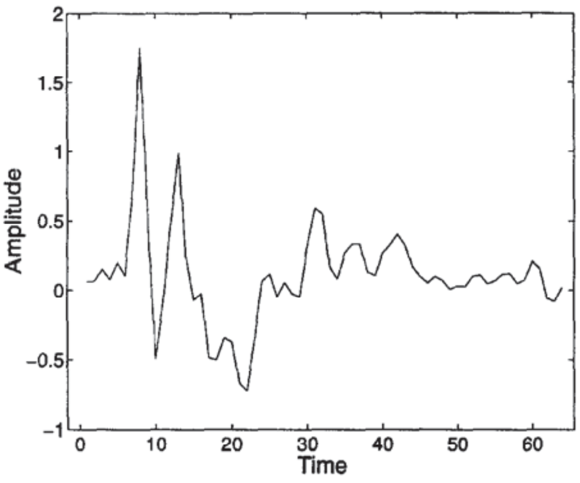


Fig. 14. Typical acoustic pressure waveform in free air from explosive charges.

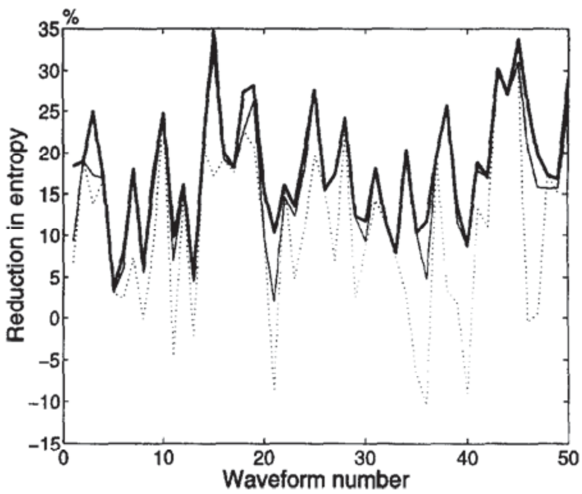


Fig. 15. Percentage of reduction in entropy over the conventional WPD using the optimal SIWPD (heavy solid line), the suboptimal SIWPD with $d = 2$ (fine solid line) and the suboptimal SIWPD with $d = 1$ (dotted line).

Table 2
Entropies attained by the conventional WPD, suboptimal SIWPD ($d < \mathrm{L}$) and optimal SIWPD ($d = \mathrm{L}$) for acoustic pressure waveforms

| Waveform # | WPD $L = 5$ | SIWPD $d = 1$ | $d = 2$ | $d = L = 5$ |
|---|---|---|---|---|
| 1 | 1.829 | 1.706 | 1.659 | 1.494 |
| 2 | 2.463 | 1.997 | 1.997 | 1.997 |
| 3 | 2.725 | 2.347 | 2.256 | 2.045 |
| 4 | 2.501 | 2.086 | 2.078 | 2.078 |
| 5 | 1.656 | 1.606 | 1.606 | 1.593 |
| 6 | 2.398 | 2.339 | 2.251 | 2.212 |
| 7 | 2.461 | 2.281 | 2.020 | 2.020 |
| 8 | 2.277 | 2.280 | 2.151 | 2.141 |
| 9 | 1.720 | 1.572 | 1.449 | 1.419 |
| 10 | 2.154 | 1.626 | 1.623 | 1.623 |
| Mean | 2.218 | 1.984 | 1.909 | 1.862 |
| Variance | 0.367 | 0.327 | 0.297 | 0.295 |

Note: The average entropy and the variance are lower when using the SIWPD, and they further decrease when $d$ is larger.

## 6. Extension to 2D wavelet packets

Referring to Section 3, the best-basis representation of a signal is rendered shift invariant by allowing a relative shift between a parent node and its respective children nodes in the expansion tree. The procedure remains essentially the same and leads to analogous results when applied to 2D signals [21,29]. In this case, a shift with respect to the origin is a vector quantity $m = (m_x, m_y)$. If we desire to generate a best-basis decomposition that remains invariant under shifts in the $X$–$Y$ plane, we must permit a, now two-dimensional, parent–children relative shift, to be determined adaptively. Let $m_p$ and $m_c$ denote the parent and children shift with respect to the origin ($x = y = 0$). The relative shift $(m_c - m_p)$ may take on any one of four values

$$m_c - m_p = \{(0, 0), (2^{-\ell}, 0), (0, 2^{-\ell}), (2^{-\ell}, 2^{-\ell})\}.$$

The value to be adapted is, once more, the one that minimizes the information cost. The proof follows along the lines charted in the one-dimensional case.

It should be stressed, however, that while the 2D expansion thus attained is shift invariant in $x$ and $y$, it is not invariant under rotation.

## 7. Concluding remarks

A library of orthonormal shifted wavelet packets is defined and a search algorithm leading to a shift invariant wavelet packet decomposition (SIWPD) introduced. When compared with the WPD algorithm proposed in [15], SIWPD is determined to be advantageous in three respects. First, it leads to a best basis expansion that is shift invariant. Second, the resulting representation is characterized by a lower information cost. Third, the complexity is controlled at the expense of the information cost.

The stated advantages, namely the shift invariance as well as the lower information cost, may prove crucial to signal compression, identification or classification applications. Furthermore, the shift-invariant nature of the information cost, renders this quantity a characteristic of the signal for a prescribed wavelet packet library. It should be possible now to quantify the relative efficiency of various libraries (i.e., various scaling function selections) with respect to a given cost function. Such a measure would be rather senseless for shift-variant decompositions.

The complexity associated with the SIWPD algorithm is $O(2^d N(L-d+2))$, (recall, $N$ denotes the length of the signal, $L$ is the number of tree decomposition levels and $d$ limits through (22) the depth of the subtrees used to estimate the optimal children nodes). One may exercise a substantial control over the complexity. The key to controlling the complexity is the built-in flexibility in the choice of $d$. Lower $d$ implies lower complexity at the expense of a higher information cost. At its lower bound, $d = 1$, the attained level of complexity, $O(NL)$, resembles that of WPD while still guaranteeing shift invariance.

The presented procedure is based on the general approach: extend the library of bases to include all their shifted versions, organize it in a tree structure and provide an efficient 'best basis' search algorithm. It is of course not limited to wavelet packets and shift invariance. Other types of bases can be used, and various extended libraries are available [9–11].

## Appendix A. Proof of Proposition 2

Let $f, g \in V_j$ be identical to within a time shift, and let $A_f$ and $A_g$ denote their respective best bases. Hence there exists $q \in \mathbb{Z}$ such that

$$g(x) = f(x - q2^{-j}). \tag{A.1}$$

We show by induction that

$$B_{\ell,n,m} \subset A_f \tag{A.2}$$

implies

$$B_{\ell,n,\tilde{m}} \subset A_g, \quad \tilde{m} = (m+q) \bmod (2^{-\ell}), \tag{A.3}$$

for all $m, n \in \mathbb{Z}_+$ and $\ell \in \mathbb{Z}_-$.

First we validate the claim for the coarsest resolution level $\ell = -L$. Suppose that

$$B_{-L,n,m_0} \subset A_f, \quad 0 \leqslant n < 2^L. \tag{A.4}$$

That is, $m = m_0$ minimizes the information cost for representing $f$ in the subspace $U_{-L,n,m}$, i.e.,

$$\operatorname*{Arg\,min}_{0 \leqslant m < 2^L} \{\mathcal{M}(B_{-L,n,m} f)\} = m_0. \tag{A.5}$$

It stems from (A.1) that

$$\begin{aligned} &\langle g(x), \psi_n[2^\ell(2^j x - m) - k]\rangle \\ &\quad = \langle f(x), \psi_n[2^\ell(2^j x - m + q) - k]\rangle, \\ &l, n, j, k, m \in \mathbb{Z}, \end{aligned} \tag{A.6}$$

and accordingly

$$\mathcal{M}(B_{\ell,n,m} g) = \mathcal{M}(B_{\ell,n,m-q} f). \tag{A.7}$$

Hence the information cost for representing $g$ in the subspace $U_{-L,n,m}$ is minimized for $m = m_0 + q$, i.e.,

$$\operatorname*{Arg\,min}_{0 \leqslant m < 2^L} \{\mathcal{M}(B_{-L,n,m} g)\} = (m_0 + q) \bmod (2^L) \tag{A.8}$$

and

$$B_{-L,n,\tilde{m}_0} \subset A_g, \quad \tilde{m}_0 = (m_0 + q) \bmod (2^L). \tag{A.9}$$

Now, suppose that the claim is true for all levels coarser than $\ell_0 (\ell_0 > -L)$, and assume that (A.2) exists for $\ell = \ell_0$. Then by (11)

$$\begin{aligned} \mathcal{M}(B_{\ell_0,n,m} f) &\leqslant \mathcal{M}(A_{\ell_0-1,2n,m_c} f) \\ &\quad + \mathcal{M}(A_{\ell_0-1,2n+1,m_c} f), \\ m_c &\in \{m, m + 2^{-\ell_0}\}. \end{aligned} \tag{A.10}$$

The inductive hypothesis together with Eq. (A.7) leads to

$$\begin{aligned} &\mathcal{M}(A_{\ell_0-1,2n+\varepsilon,m_c} f) = \mathcal{M}(A_{\ell_0-1,2n+\varepsilon,m_c+q} g), \\ &\varepsilon \in \{0, 1\}. \end{aligned} \tag{A.11}$$

Consequently,

$$\begin{aligned}&\mathscr{M}(B_{\ell_0,n,m+q}\,g)\\&\quad\leqslant \mathscr{M}(A_{\ell_0-1,2n,m_c+q}\,g)+\mathscr{M}(A_{\ell_0-1,2n+1,m_c+q}\,g),\\&\quad m_c\in\{m,m+2^{\ell_0}\},\end{aligned} \tag{A.12}$$

and again by (11) we have

$$B_{\ell_0,n,\tilde{m}}=A_g,\quad \tilde{m}=(m+q)\,\mathrm{mod}\,(2^{-\ell_0}) \tag{A.13}$$

proving as well the validity of the claim for $\ell_0$. Thus, $A_f$ and $A_g$ are *identical to within a time shift*.

## References


[1] F. Bao, N. Erdol, The optimal wavelet transform and translation invariance, in: Proc. 19th IEEE Internat. Conf. Acoust. Speech Signal Process. Adelaide, 19–22 April 1994, pp. III.13–III.16.

[2] S.A. Benno, J.M.F. Moura, Nearly shiftable scaling functions, in: Proc. 20th IEEE Internat. Conf. Acoust. Speech Signal Process. Detroit, MS, 8–12 May 1995, pp. 1097–1100.

[3] Z. Berman, J.S. Baras, Properties of the multiscale maxima and zero-crossings representations, IEEE Trans. Signal Process. 41 (12) (December 1993) 3216–3231.

[4] G. Beylkin, On the representation of operators in bases of compactly supported wavelets, SIAM J. Numer. Anal 6 (6) (December 1992) 1716–1740.

[5] P.J. Burt, Fast filter transforms for image processing, Comput. Graph. Image Process. 16 (1981) 20–51.

[6] T. Chang, C.J. Kuo, Texture analysis and classification with tree-structured wavelet transform, IEEE Trans. Image Process. 2 (October 1993) 429–441.

[7] L. Cohen, Time-frequency distributions – a review, Proc. IEEE 77 (7) (July 1989) 941–981.

[8] I. Cohen, S. Raz, D. Malah, Shift invariant wavelet packet bases, in: Proc. 20th IEEE Internat. Conf. Acoustics, Speech Signal Process., Detroit, Michigan, 8–12 May 1995, pp. 1081–1084.

[9] I. Cohen, S. Raz, D. Malah, Shift-invariant adaptive local trigonometric decomposition, in: Proc. 4th European Conf. Speech Commun. Technology, Madrid, Spain, 18–21 September 1995, pp. 247–250.

[10] I. Cohen, S. Raz, D. Malah, Shift-invariant adaptive representations in libraries of bases, Technical Report, Technion – Israel Institute of Technology, Haifa, Israel, December 1995.

[11] R.R. Coifman, D.L. Donoho, Translation-invariant denoising, in: A. Antoniadis and G. Oppenheim (Ed.), Wavelet and Statistics, Lecture Notes in Statistics, Springer, Berlin, 1995, pp. 125–150.

[12] R.R. Coifman, Y. Meyer, Orthonormal wave packet bases, Yale University, August 1989 (in: ftp pascal.math.yale.edu/pub/wavelets/wavepkt.tex).

[13] R.R. Coifman, Y. Meyer, S. Quake, M.V. Wickerhauser, Signal processing and compression with wave packets, in: Proc. Conf. Wavelets, Marseilles, Spring 1989.

[14] R.R. Coifman, Y. Meyer, V. Wickerhauser, Size properties of wavelet packets, in: M.B. Ruskai et al. (Eds.), Wavelets and Their Applications, Jones and Bartlett, Boston, 1992, pp. 453–470.

[15] R.R. Coifman, M.V. Wickerhauser, Entropy-based algorithms for best basis selection, IEEE Trans. Inform. Theory 38 (March 1992) 713–718.

[16] R.R. Coifman, M.V. Wickerhauser, Adapted waveform analysis as a tool for modeling, feature extraction, and denoising, Optical Engineering 33 (7) (July 1994) 2170–2174.

[17] I. Daubechies, Orthonormal bases of compactly supported wavelets, Commun. Pure Appl. Math. 41 (1988) 909–996.

[18] I. Daubechies, Ten Lectures on Wavelets, CBMS-NSF Regional Conf. Ser. Appl. Math., SIAM, Philadelphia, Pennsylvania, 1992.

[19] I. Daubechies, Orthonormal bases of compactly supported wavelets, II. Variations on a theme, SIAM J. Math. Anal. 24 (1993) 499–519.

[20] G. Davis, S. Mallat, Z. Zhang, Adaptive time-frequency decompositions, Opt. Eng. 33 (7) (July 1994) 2183–2191.

[21] S. Del Marco, P. Heller, J. Weiss, An M-band 2-dimensional translation-invariant wavelet transform and applications, in: Proc. 20th IEEE Internat. Conf. Acoust. Speech Signal Process., Detroit, Michigan, 8–12 May 1995, pp. 1077–1080.

[22] S.P. Del Marco, J. Weiss, K. Jagler, Wavepacket-based transient signal detector using a translation invariant wavelet transform, Proc. SPIE 2242 (1994) 792–802.

[23] C. Herley, J. Kovačević, K. Ramchandran, M. Vetterli, Tilings of the time-frequency plane: Construction of arbitrary orthogonal bases and fast tiling algorithms, IEEE Trans. Signal Process 41 (December 1993) 3341–3359.

[24] C. Herley, Z. Xiong, K. Ramchandran, M.T. Orchard, An efficient algorithm to find a jointly optimal time-frequency segmentation using time-varying filter banks, in: Proc. 20th IEEE Internat. Conf. Acoust. Speech Signal Process., Detroit, MI, 8–12 May 1995, pp. 1516–1519.

[25] R. Hummel, R. Moniot, Reconstructions from zero crossings in scale space, IEEE Trans. Acoust. Speech Signal Process. 37 (December 1989) 2111–2130.

[26] B. Jawerth, Y. Liu, W. Sweldens, Signal compression with smooth local trigonometric bases, Optical Eng. 33 (7) (July 1994) 2125–2135.

[27] R. Kronland-Martinet, J. Morlet, A. Grossman, Analysis of sound patterns through wavelet transforms, Internat J. Pattern Rec. Art. Intell. 1 (1987) 273–301.

[28] A. Laine, J. Fan, Texture classification by wavelet packet signatures, IEEE Trans. Pattern Anal. Mechine Intell. 15 (11) (November 1993) 1186–1191.

[29] J. Liang, T.W. Parks, A two-dimensional translation invariant wavelet representation and its application, in: Proc. Internat. Conf. Image Process., Austin, TX, 13–16 November 1994, pp. 66–70.

[30] J. Liang, T.W. Parks, A translation invariant wavelet representation algorithm with applications, IEEE Trans. Signal Process. 44 (2) (February 1996) 225–232.
[31] S.G. Mallat, A theory for multiresolution signal decomposition: The wavelet decomposition, IEEE Trans. Pattern Anal. Machine Intell. 11 (July 1989) 674–693.
[32] S. Mallat, Zero crossings of a wavelet transform, IEEE Trans. Inform. Theory 37 (July 1991) 1019–1033.
[33] S. Mallat, W.L. Hwang, Singularity detection and processing with wavelets, IEEE Trans. Inform. Theory 38 (2) (March 1992) 617–643.
[34] S. Mallat, S. Zhong, Characterization of signals from multiscale edges, IEEE Trans. Pattern Anal. Machine Intell. 14 (July 1992) 710–732.
[35] S. Mallat, Z. Zhang, Matching pursuit with time-frequency dictionaries, IEEE Trans. Signal Process. 41 (December 1993) 3397–3415.
[36] G.P. Nason, B.W. Silverman, The stationary wavelet transform and some statistical applications, in: A. Antoniadis and G. Oppenheim (Eds), Wavelet and Statistics, Lecture Notes in Statistics, Springer, Berlin, 1995, pp. 281–300.
[37] J.-C. Pesquet, H. Krim, H. Carfantan, J.G. Proakis, Estimation of noisy signals using time-invariant wavelet packets, in: Proc. Asilomar Conf., Monterey, CA, USA, Vol. 1, November 1993, pp. 31–34.
[38] K. Ramchandran, M. Vetterli, Best wavelet packet bases in a rate-distortion sense, IEEE Trans. Image Process. 2 (April 1993) 160–175.
[39] O. Rioul, P. Duhamel, Fast algorithms for discrete and continuous wavelet transforms, IEEE Trans. Inform Theory 38 (March 1992) 569–586.
[40] O. Rioul, M. Vetterli, Wavelets and signal processing, IEEE Signal Process. Mag. 8 (October 1991) 14–38.
[41] N. Saito, Local feature extraction and its applications using a library of bases, Ph.D. Dissertation, Yale Univ., New Haven, December 1994.
[42] N. Saito, G. Beylkin, Multiresolution representation using the auto-correlation functions of compactly supported wavelets, IEEE Trans. Signal Process. 41 (December 1993) 3584–3590.
[43] E.P. Simoncelli, W.T. Freeman, E.H. Adelson, D.J. Heeger, Shiftable multiscale transforms, IEEE Trans. Inform. Theory, 38 (2) (March 1992) 587–607.
[44] M. Vetterli, Wavelet and filter banks for discrete-time signal processing, in: M.B. Ruskai et al. (Eds.), Wavelets and Their Applications, Jones and Bartlett, Boston, 1992, pp. 17–52.
[45] M. Vetterli, C. Herley, Wavelets and filter banks: Theory and design, IEEE Trans. Signal Process. 40 (September 1992) 2207–2232.
[46] G.G. Walter, Wavelets and Other Orthogonal Systems With Applications, CRC Press, Boca Raton, FL, 1994.
[47] E. Wesfreid, M.V. Wickerhauser, Adapted local trigonometric transforms and speech processing, IEEE Trans. Signal Process. 41 (12) (December 1993) 3596–3600.
[48] M.V. Wickerhauser, Acoustic signal compression with wavelet packets, in: C.K. Chui (Ed.), Wavelets – A Tutorial in Theory and Applications, Academic Press, Boston, 1992, pp. 679–700.
[49] M.V. Wickerhauser, Adapted Wavelet Analysis from Theory to Software, AK Peters, Wellesley, MA, 1994.